Griffiths singularities in the disordered phase of a quantum Ising spin glass

H. Rieger
HLRZ, Forschungszentrum Jülich, 52425 Jülich, Germany
and Institut für Theoretische Physik, Universität zu Köln, 50937 Köln, Germany

A. P. Young
Department of Physics, University of California, Santa Cruz, California 95064
(Received 22 December 1995)

We study a model for a quantum Ising spin glass in two space dimensions by Monte Carlo simulations. In the disordered phase at $T=0$, rare strongly correlated regions give rise to strong Griffiths singularities, as originally found by McCoy for a one-dimensional model. We find that there are power law distributions of the local susceptibility and local nonlinear susceptibility, which are characterized by a smoothly varying dynamical exponent z. Over a range of the disordered phase near the quantum transition, the local nonlinear susceptibility diverges. The local susceptibility does not diverge in the disordered phase but does diverge at the critical point. Approaching the critical point from the disordered phase, the limiting value of z seems to equal its value precisely at criticality, even though the physics of these two cases seems rather different.
[S0163-1829(96)04430-X]

I. INTRODUCTION

A feature of disordered systems which has no counterpart in pure systems, is that rare regions, which are more strongly correlated than the average, can play a significant role. For classical magnetic systems, Griffiths[1] showed that such regions lead to a free energy which is a nonanalytic function of the magnetic field at temperatures below the transition temperature of the pure system. However, for the static properties of a classical system, the Griffiths singularities are very weak; just essential singularities.[2] By contrast, Griffiths singularities are much more spectacular for quantum phase transitions at $T=0$, especially for systems with a broken *discrete* symmetry. This was first found by McCoy[3] for a one-dimensional model, the one-dimensional random transverse-field Ising model, which has recently been studied in more detail by Fisher.[4] In this model Griffiths singularities dominate not only the disordered phase but also the critical region.[3–7] One finds very broad distributions of various quantities including the local susceptibility and the energy gap, and a dynamical exponent, z, which is infinite at the critical point. In the disordered phase, the distribution of local susceptibilities is found to be a power law, in which the power can be related[7] to a continuously varying dynamical exponent,[4] which diverges at criticality. The *average* susceptibility diverges when $z>1$, i.e., over a finite region of the disordered phase in the vicinity of the critical point, a result first found many years ago by McCoy.[3]

Many of these surprising results of the one-dimensional model, such as the power law distribution of susceptibilities in the disordered phase, are expected to hold more generally.[8] However, it is not clear whether the average susceptibility will diverge in the disordered phase for dimension, d, greater than 1, or whether this is a special feature of $d=1$. Here we investigate Griffiths singularities for a *two*-dimensional quantum Ising *spin glass* system by Monte Carlo simulations. The one-dimensional model has no frustration and so is a random ferromagnet rather than a spin glass. In higher dimension, though, one can have frustration, which, together with randomness, gives spin glass behavior. The main features of Griffiths singularities are expected to be similar regardless of whether or not one has frustration. Our motivation for studying a spin glass here, rather than a random ferromagnet, is experimental work[9] on a quantum spin glass system. This did not find the expected strong divergence in the nonlinear susceptibility at the quantum phase transition. By contrast, subsequent numerical simulations[10,11] did find a rather strong divergence, comparable with that at the classical spin glass transition. Hence it seems worth investigating whether this discrepancy might be due to Griffiths singularities causing the nonlinear susceptibility to diverge even in the disordered phase, thus making the location of the transition difficult in the experiments. While the earlier simulations[10] concentrated on the *critical point*, here we focus mainly on the *disordered phase*. Somewhat less detailed results on the two-dimensional spin glass have also been reported in parallel work by Guo *et al.*,[12] who, additionally, performed calculations in three dimensions.

II. THE MODEL

The two-dimensional quantum Ising spin glass in a transverse field[13] is has the following Hamiltonian:

$$\widetilde{\mathcal{H}}_{\mathrm{QM}} = -\sum_{\langle i,j\rangle} \widetilde{J}_{ij}\sigma_i^z\sigma_j^z - \Gamma\sum_i \sigma_i^x, \tag{1}$$

where the $\{\sigma_i^\alpha\}$ are Pauli spin matrices, the $\widetilde{J}_{ij}$ are quenched random interaction strengths, and Γ is an external transverse field. A system described by this Hamiltonian undergoes a quantum phase transition at zero temperature, $T=0$, from a paramagnetic (or spin liquid) phase to a spin glass phase for some critical field strength Γ_c.[10] As is described elsewhere[10,11] this model can be mapped onto an effective

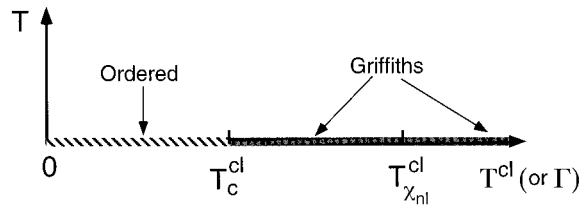

FIG. 1. The phase diagram of the two-dimensional quantum Ising spin glass. The horizontal axis can be thought of as $T^{\rm cl}$ if one is using the effective classical Hamiltonian in Eq. (2) or Γ if one is using the original quantum Hamiltonian in Eq. (1). There is a critical point at $T^{\rm cl}=T_c^{\rm cl}$ For $T^{\rm cl}<T_c^{\rm cl}$ there is a spin glass ordered phase. For $T^{\rm cl}>T_c^{\rm cl}$ there is no spin glass order but there are Griffiths singularities. In the region $T_c^{\rm cl}<T^{\rm cl}<T_{\chi_{\rm nl}}^{\rm cl}$ the Griffiths singularities are sufficiently strong that the average nonlinear susceptibility diverges as the (real) temperature tends to zero. For $T^{\rm cl}>T_{\chi_{\rm nl}}^{\rm cl}$ the average nonlinear susceptibility stays finite in the zero temperature limit.

classical Hamiltonian in two space plus one imaginary time dimensions, with disorder that is perfectly correlated along the imaginary time axis. This classical Hamiltonian is

$$\mathcal{H}=-\sum_{\tau}\sum_{\langle i,j\rangle}J_{ij}S_i(\tau)S_j(\tau)-\sum_{\tau,i}S_i(\tau)S_i(\tau+1), \quad (2)$$

where the Ising spins, $S_i(\tau)$, take values ± 1, i and j refer to the sites on an $L\times L$ spatial lattice, while τ denotes a time slice, $\tau=1,2,\ldots,L_\tau$. The number of time slices, L_τ, is proportional to the inverse of the temperature, T, of the original quantum system in Eq. (1). Periodic boundary conditions are applied in all directions. The model is simulated at an effective classical ''temperature'' $T^{\rm cl}$, which controls the amount of order in the spins. Of course, $T^{\rm cl}$, is not the real temperature T, which is zero at the transition, but is rather a measure of the strength of the *quantum* fluctuations. Increasing $T^{\rm cl}$ therefore corresponds to increasing the transverse field Γ, in the quantum Hamiltonian, Eq. (1). The nearest neighbor interactions J_{ij} are independent of τ, because they are quenched random variables, and are chosen independently from a Gaussian distribution with zero mean and standard deviation unity, i.e.,

$$[J_{ij}]_{\rm av}=0,$$

$$[J_{ij}^2]_{\rm av}=1, \quad (3)$$

where $[\cdots]_{\rm av}$ denotes an average over the disorder. Statistical mechanics averages for a given sample will be denoted by angular brackets, i.e. $\langle\cdots\rangle$. The interactions between time slices are ferromagnetic and taken to be nonrandom with strength unity.

The phase diagram of the model is sketched in Fig. 1. Because we are dealing with a two-dimensional lattice, there is no finite-temperature spin glass transition,[14] and the region with spin glass order therefore lies entirely along the $T=0$ axis in the region $0\leqslant T^{\rm cl}<T_c^{\rm cl}$ where $T_c^{\rm cl}$ denotes the critical point. In earlier work[10] we found that

$$T_c^{\rm cl}=3.275\pm 0.025. \quad (4)$$

III. THEORY

Griffiths singularities arise from localized regions which are more correlated than the average. They do not have large spatial correlations, but give rise to singularities because of large correlations in imaginary time. To focus on these time correlations, it is simplest to study quantities that are completely *local* in space, i.e., are just on a single site. We shall be particularly interested in the local susceptibility,

$$\chi^{(\rm loc)}=\frac{\partial}{\partial h_i}\langle\sigma_i^z\rangle, \quad (5)$$

where h_i is a local field on site i. In the imaginary time formalism this can be evaluated from

$$\chi^{(\rm loc)}=\sum_{\tau=1}^{L_\tau}\langle S_i(0)S_i(\tau)\rangle. \quad (6)$$

Since the divergent response function at a conventional spin glass transition is the nonlinear susceptibility,[14] it is also interesting to study the local nonlinear susceptibility, given by

$$\chi_{\rm nl}^{(\rm loc)}=\frac{\partial^3}{\partial h_i^3}\langle\sigma_i^z\rangle, \quad (7)$$

which can be determined in the simulations from

$$\chi_{\rm nl}^{(\rm loc)}=-\frac{1}{6L_\tau}(\langle m_i^4\rangle-3\langle m_i^2\rangle^2), \quad (8)$$

where

$$m_i=\sum_{\tau=1}^{L_\tau}S_i(\tau). \quad (9)$$

We consider distributions of $\chi^{(\rm loc)}$ and $\chi_{\rm nl}^{(\rm loc)}$ obtained both by measuring at different sites in a given sample, and by taking many samples with different realizations of the disorder.

A. Disordered phase

In the disordered phase the distributions of $\chi^{(\rm loc)}$ and $\chi_{\rm nl}^{(\rm loc)}$ will be very broad with a power law variation at large values. Physically this comes from regions which are locally ordered. The probability of having such a region is exponentially small in its volume, V, but, when it occurs, there is an exponentially large relaxation time,[8] because, to invert the spins in this region at some imaginary time one has to insert a domain wall of size V, for which the Boltzmann factor is exponentially small in V, as is sketched in Fig. 2. The combination of an exponentially large result happening with exponentially small probability gives a broad distribution of results in complete analogy to the effect of the Griffiths phase on the dynamics in *classical* random magnets.[15,16] In the latter case the volume to surface ratio determines the resulting probability distribution for the logarithm of relaxation times. In contrast to this the extra dimension present in the quantum problem gives rise to a volume to volume ratio instead (cf. Fig. 2), which leads to a power law distribution of correlation lengths in the imaginary time direction. The

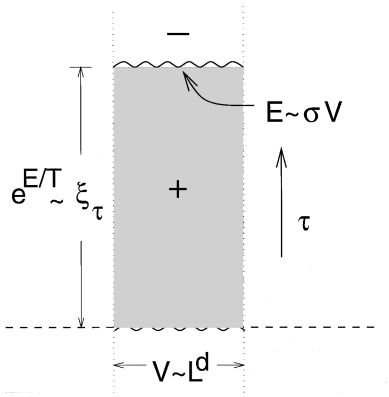

FIG. 2. The strongly coupled space region (cluster) of volume $V \sim L^d$ tends to order (locally) the spins along the imaginary time (τ) direction, indicated by the plus and minus sign meaning a spin orientation parallel (plus) or antiparallel (minus) with respect to the ground state configuration of the isolated cluster. The insertion of a domain wall costs an energy $E \sim \sigma V$, where σ is a surface tension (note that the couplings in the τ direction are all ferromagnetic). This event occurs with a probability $\exp(-E/T^{\rm cl})$, resulting in the exponentially large (imaginary) correlation time $\xi_\tau \sim \exp(\sigma L^d/T^{\rm cl})$.

power depends on the microscopic details and so is expected to vary smoothly throughout the Griffiths phase.

We can relate the power in the distribution to a dynamical exponent, defined in the disordered phase, as follows.[7] The excitations which give rise to a large $\chi^{(\rm loc)}$ at $T=0$ are well localized and so we assume that their probability is proportional to the spatial volume, L^d. These excitations have a very small energy gap, $\Delta E = E_1 - E_0$, where E_0 is the ground state energy of the quantum system and E_1 is the first excited state. This small gap is responsible for the large susceptibility because the latter is essentially proportional to the inverse of the gap because the matrix elements which enter $\chi^{(\rm loc)}$ do not have very large variations. Since there is no characteristic energy gap it is most sensible to use logarithmic variables. Hence, if the power in the distribution of $\ln\Delta E$ is λ, say, then we have

$$\begin{aligned} P(\ln\Delta E) &\equiv \Delta E \widetilde{P}(\Delta E) \\ &\sim L^d \Delta E^{\lambda} \\ &= (L \Delta E^{1/z})^d, \end{aligned} \tag{10}$$

where the last line defines the dynamical exponent, z, in the conventional way as the power relating a time scale to a length scale. Comparing the last two expressions we see that

$$\lambda = \frac{d}{z}. \tag{11}$$

Hence the tail of the distribution of ΔE has the form

$$\ln[P(\ln\Delta E)] = \frac{d}{z}\ln\Delta E + \text{ const.} \tag{12}$$

Since the local susceptibility is proportional to the inverse of the gap, the power law tail of its distribution should be given by

$$\ln[P(\ln\chi^{(\rm loc)})] = -\frac{d}{z}\ln\chi^{(\rm loc)} + \text{ const.} \tag{13}$$

The nonlinear susceptibility involves three integrals over time, whereas the linear susceptibility only involves one. Hence we assume that the distribution of $\chi_{\rm nl}^{(\rm loc)}$ is similar to that of $(\chi^{(\rm loc)})^3$, which leads to the following power law tail in the distribution:

$$\ln[P(\ln\chi_{\rm nl}^{(\rm loc)})] = -\frac{d}{3z}\ln\chi_{\rm nl}^{(\rm loc)} + \text{ const.} \tag{14}$$

Hence there should be a factor of 3 between the powers in the distributions of $\ln\chi^{(\rm loc)}$ and $\ln\chi_{\rm nl}^{(\rm loc)}$ We shall see that this prediction is confirmed by the numerics. As a result, one can characterize *all* the Griffiths singularities in the disordered phase by a *single* dynamical exponent, z, which varies smoothly throughout the Griffiths phase.

The *average* uniform susceptibility will diverge, in the disordered phase, at the same point as the average local susceptibility because spatial correlations are short range and so cannot contribute to a divergence. From Eq. (13) we see that this happens when

$$z > d. \tag{15}$$

Similarly, according to Eq. (14), the average nonlinear susceptibility will diverge when

$$z > \frac{d}{3}. \tag{16}$$

One can also infer the nature of the divergence of $\chi_{\rm nl}^{(\rm loc)}$ and $\chi^{(\rm loc)}$ as the (real) temperature T tends to zero, see Fig. 1. For $\chi^{(\rm loc)}$ we expect that the distribution in Eq. (13) will be cut off at $\chi^{(\rm loc)} \sim T^{-1}$ which gives

$$[\chi^{(\rm loc)}]_{\rm av} \sim T^{d/z-1}. \tag{17}$$

For $\chi_{\rm nl}^{(\rm loc)}$ we expect that the cutoff will be at of order T^{-3}, which, together with Eq. (14) gives

$$[\chi_{\rm nl}^{(\rm loc)}]_{\rm av} \sim T^{d/z-3}. \tag{18}$$

The global nonlinear susceptibility will diverge in the same way, possibly with logarithmic corrections, as occurs in the one-dimensional random ferromagnet.[4]

The dynamical exponent will tend to some limit as the critical point is approached. It is interesting to ask whether this limit will be the same as the value of z precisely at criticality. On the face of it, there does not seem any reason why they should be equal, since z in the disordered phase is determined by rare compact clusters, whereas z at criticality is determined by fluctuations on large length scales of order of the (divergent) correlation length. Nonetheless, for the 1D random ferromagnet, they *are* both equal (to infinity). For the 2D spin glass we shall also find that these two values are numerically close, and may well be equal (though finite).

B. The critical point

We expect that the distribution of $\chi^{(\rm loc)}$ will also have a power law at the critical point just as it does in the disor-

dered phase. To deduce the exponent, note that the average time dependent correlation function at criticality is given by scaling as[10,11]

$$[\langle S_i(0)S_i(\tau)\rangle]_{\rm av}\sim\frac{1}{\tau^{\beta/(\nu z)}}, \tag{19}$$

where

$$\frac{\beta}{\nu}=\frac{d+z-2+\eta}{2} \tag{20}$$

is the order parameter exponent and ν is the correlation length exponent.

Since the average local susceptibility is just the integral of this over τ, it follows that the distribution of $\ln\chi^{(\rm loc)}$ must have the same power, i.e.,

$$\ln[P(\ln\chi^{(\rm loc)})]=-\left(\frac{\beta}{\nu z}\right)\ln\chi^{(\rm loc)}+\text{ const} \tag{21}$$

at criticality. In earlier work[10] we found $z=1.5, \eta=0.5$, so numerically $\beta/(\nu z)$ is about 2/3.

Integrating Eq. (19) over τ from 0 to T^{-1}, one sees that the average susceptibility (which is the same as the average local susceptibility for a model with a symmetric distribution of interactions, such as that used here) diverges as $T\to 0$ like

$$[\chi]_{\rm av}\sim T^{\beta/z\nu-1}, \tag{22}$$

at criticality. Similarly the average local nonlinear susceptibility will diverge like[10,11]

$$[\chi_{\rm nl}^{(\rm loc)}]_{\rm av}\sim T^{2\beta/z\nu-3}, \tag{23}$$

at criticality. The global nonlinear susceptibility will have a stronger divergence at criticality[10]:

$$[\chi_{\rm nl}]_{\rm av}\sim T^{(2\beta-d\nu)/z\nu-3}. \tag{24}$$

Note that Eqs. (22)–(24) refer to the situation in which $T^{\rm cl}$ is set to the critical value $T_c^{\rm cl}$ and the real temperature tends to zero, see Fig. 1.

IV. RESULTS IN THE DISORDERED PHASE

We use standard Monte Carlo methods to simulate the model in Eq. (2). Except where noted, 2560 realizations of the disorder were averaged over. The simulations were done on parallel computers: a Parsytec GCel1024 with 1024 nodes (T805 transputers) and a Paragon XP/S10 with 140 nodes (i860XP microprocessors). Massively parallel machines with many medium-sized nodes (in terms of memory) are ideal for the problem considered here: as long as one physical system fits into the RAM of one processor one only has to set up a farm topology to distribute the initial seed for the random number generators and to collect the results for the different realizations at the end of the simulation. Apart from that, no communication between processors is needed, so the parallelization is perfectly efficient; the gain in speed is directly proportional to the number of nodes.

The distributions of $\ln\chi^{(\rm loc)}$ and $\ln\chi_{\rm nl}^{(\rm loc)}$ at $T^{\rm cl}=3.7$ and 3.5 (both in the disordered phase) are shown in Figs. 3–6. There is a straight line region for large values as expected,

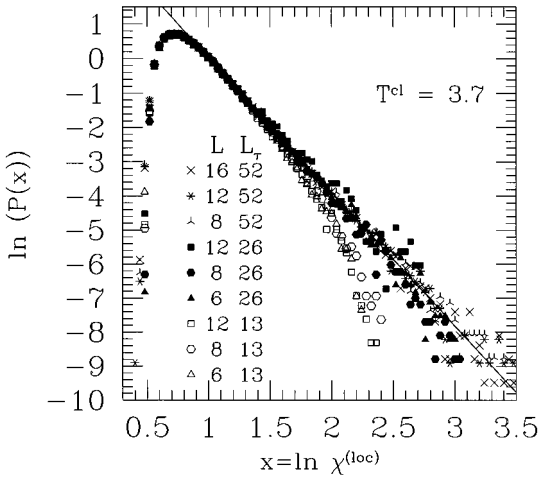

FIG. 3. The log of the distribution of the log of the local susceptibility for $T^{\rm cl}=3.7$ for different values of L and L_τ. There is no significant dependence on L and the data are also independent of L_τ at small $\chi^{(\rm loc)}$. Increasing L_τ seems to simply extend the range over which the data lies on a straight line. The solid line is a fit to the straight line region of the data and has slope -3.92 which gives $z=0.51$ from Eq. (13).

which is independent of L, and the only dependence on L_τ is that the tail extends further for larger L_τ. This is not surprising since there is a cutoff due to the finite number of time slices at $\chi^{(\rm loc)}=L_\tau$ and $\chi_{\rm nl}^{(\rm loc)}=L_\tau^3$ At both temperatures one sees that the values of z obtained from $\chi^{(\rm loc)}$ and $\chi_{\rm nl}^{(\rm loc)}$ are in reasonably good agreement with each other. At $T^{\rm cl}=3.7$, we find that $z\simeq 0.51$, from the data for $\chi^{(\rm loc)}$ and $z\simeq 0.54$ from data for $\chi_{\rm nl}^{(\rm loc)}$ Hence, according to Eq. (16), the average $\chi_{\rm nl}^{(\rm loc)}$ does not diverge at $T^{\rm cl}=3.7$ because $z<2/3$. At $T^{\rm cl}=3.5$, we find $z\simeq 0.71$ from the data for $\chi^{(\rm loc)}$ and $z\simeq 0.76$ from data for $\chi_{\rm nl}^{(\rm loc)}$. Hence, the average $\chi_{\rm nl}^{(\rm loc)}$ *does* diverge at $T^{\rm cl}=3.5$.

Figure 7 shows the values of z at various points in the

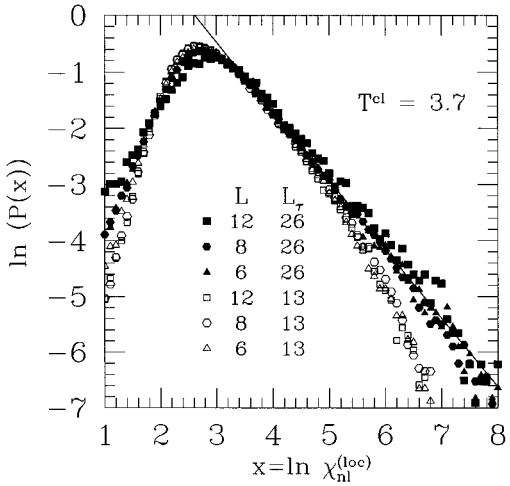

FIG. 4. Similar to Fig. 3 but for the local nonlinear susceptibility. The straight line has slope -1.23 which gives $z=0.54$ from Eq. (14), in quite good agreement with the fit to the data in Fig. 3. Since the slope is more negative than -1, or equivalently $z<2/3$, the average nonlinear susceptibility does not diverge at this point.

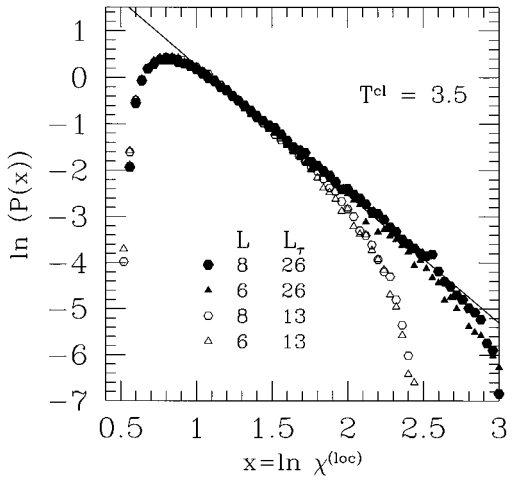

FIG. 5. Similar to Fig. 3 but for $T^{cl}=3.5$. The straight line has slope -2.78 which gives $z=0.71$ from Eq. (13).

disordered phase. In all cases there is good agreement between the estimates from the data for $\chi^{(loc)}$ and $\chi_{nl}^{(loc)}$. From these data we find that the average nonlinear susceptibility diverges, in the disordered phase, for

$$T_c^{cl} \leqslant T^{cl} \leqslant T_{\chi_{nl}}^{cl}, \tag{25}$$

where

$$T_{\chi_{nl}}^{cl} \simeq 3.56 \tag{26}$$

and $T_c^{cl} \simeq 3.275$ from earlier work.[10] Note that, according to Fig. 7 and Eq. (15), the average linear susceptibility does not diverge anywhere in the disordered phase. It appears that the value of z precisely at criticality may equal the value as the critical point is approached from the disordered phase, even though it is not clear that they have to be equal.

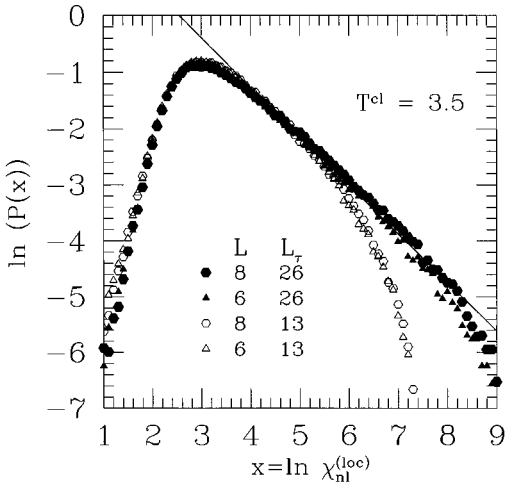

FIG. 6. Similar to Fig. 5 but for the local nonlinear susceptibility. The straight line has slope -0.87 which gives $z=0.76$ from Eq. (14), in fair agreement with the fit to the data in Fig. 5. Since the slope is greater than -1, or equivalently $z>2/3$, the average nonlinear susceptibility does diverge at this point.

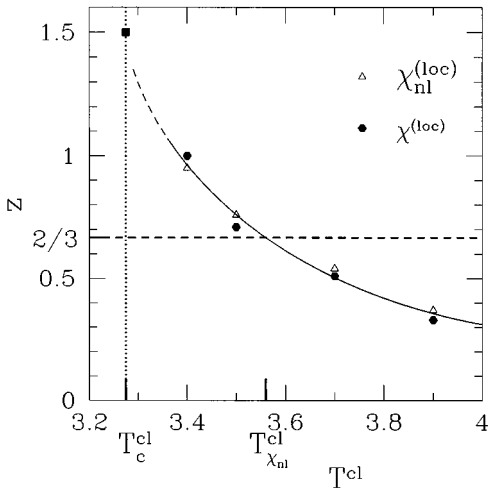

FIG. 7. The dynamical exponent z, obtained by fitting the distributions of $\chi^{(loc)}$ and $\chi_{nl}^{(loc)}$ to Eqs. (13) and (14), is plotted for different values of T^{cl}. The estimates obtained from data for $\chi^{(loc)}$ are shown by the triangles and the estimates from the data for $\chi_{nl}^{(loc)}$ are shown by the hexagons. The two are in good agreement. The dotted vertical line indicates the critical point, obtained in Ref. 10 and the solid square indicates the estimate of z at the critical point. The dashed line is $z=2/3$; the average nonlinear susceptibility diverges for z larger than this, i.e., $T^{cl} > T_{\chi_{nl}}^{cl} \simeq 3.56$. The solid curve is just a guide to the eye.

V. RESULTS AT THE CRITICAL POINT

From finite size scaling, the average uniform susceptibility (which is the same as the average local susceptibility for a model with a symmetric distribution of interactions, such as that used here) varies with L and L_τ at the critical point according to[10,11]

$$[\chi]_{av} = L^x \tilde{\chi}\left(\frac{L_\tau}{L^z}\right), \tag{27}$$

where

$$x = z - \frac{\beta}{\nu} = \frac{z-d+2-\eta}{2}. \tag{28}$$

In earlier work[10] we found $z \simeq 1.5$, $\eta \simeq 0.5$, $\nu \simeq 1.0$, and $\beta \simeq 1.0$ so $(z-d+2-\eta)/2 \simeq 1/2$. The earlier work concentrated on a fixed value of L_τ/L^z, which we call the ''aspect ratio.'' Here we investigate whether Eq. (27) is satisfied for a range of aspect ratios. The data, shown in Fig. 8, do indeed collapse well with the expected values of the exponents. For $L_\tau/L^z \ll 1$, which corresponds to a large system at finite temperature, the dependence on L should drop out, and so, from $L_\tau \propto T^{-1}$, one recovers Eq. (22). Using the numerical values of the exponents gives

$$[\chi]_{av} \sim T^{-1/3}. \tag{29}$$

Thus the average susceptibility diverges at the critical point, though we have seen above that it does not diverge in the disordered phase.

The average local nonlinear susceptibility is expected to vary at the critical point as

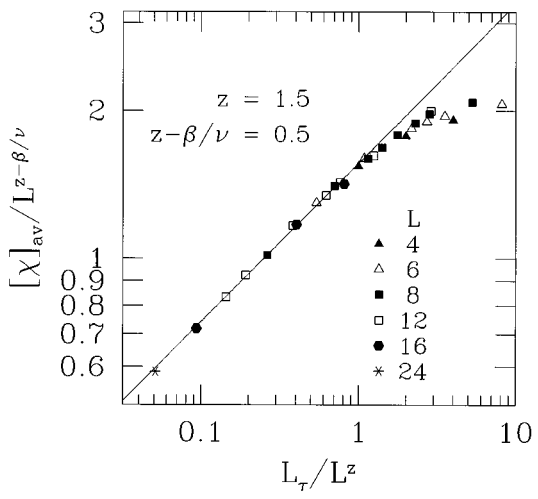

FIG. 8. A scaling plot of the data for the average susceptibility at $T^{\mathrm{cl}}=3.30$, which is the critical point, to within our errors; see Eq. (4). The plot assumes the form in Eq. (27) with the exponent values deduced in earlier work (Ref. 10), i.e. $z=1.5, \beta/\nu=1$. It is seen that the plot works well. The solid line, which fits the data for $L_\tau/L^z<0.8$ has slope 0.5/1.5=1/3 as expected, since the average susceptibility should be independent of L in this limit. The power 1/3 gives the divergence as $T\to 0$ at criticality; see Eq. (29).

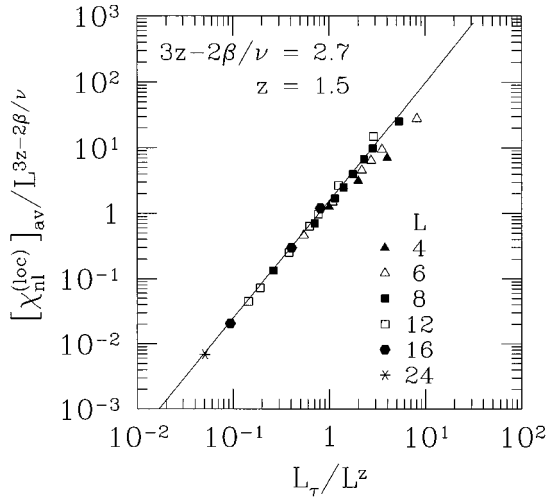

FIG. 9. A finite size scaling plot of the average local nonlinear susceptibility, according to Eq. (30), at $T^{\mathrm{cl}}=3.30$, very close to the critical point. The solid line, which fits the data for small L_τ/L^z has slope 2.7/1.5=1.8 as expected, since the average local nonlinear susceptibility should be independent of L in this limit. The power 1.8 gives the divergence as $T\to 0$, and this value agrees well with estimates from the earlier estimates of exponent (Ref. 10), see Eq. (32).

$$[\chi_{\mathrm{nl}}^{(\mathrm{loc})}]_{\mathrm{av}}=L^{y}\tilde{\chi}_{\mathrm{nl}}^{(\mathrm{loc})}\left(\frac{L_\tau}{L^z}\right), \tag{30}$$

where[10]

$$y=3z-\frac{2\beta}{\nu}. \tag{31}$$

With the numerical values of the exponents found earlier,[10] one has $y\simeq 2.5$. For $L_\tau/L^z\ll 1$, which corresponds to a large system at finite temperature, the dependence on L should drop out, and so one recovers Eq. (23). Using the numerical values of the exponents gives

$$[\chi_{\mathrm{nl}}^{(\mathrm{loc})}]_{\mathrm{av}}\sim T^{-5/3}. \tag{32}$$

The data, shown in Fig. 9, collapse well for L_τ/L^z not too large provided $y/z\simeq 1.8$, which gives a $T^{-1.8}$ divergence, close to the prediction in Eq. (32). However, the data collapse is not as good for larger values of L_τ with $z=1.5$. Data in this region are difficult to equilibrate, which may be the cause of the discrepancy. It should be noted, though, that a better data collapse is obtained for larger values of z. However, the data for $[\chi]_{\mathrm{av}}$ do not scale well with a significantly larger value of z.

We show results for the distribution of $\chi^{(\mathrm{loc})}$ at the critical point, $T^{\mathrm{cl}}=3.3$, in Fig. 10. Unlike the data in the disordered phase, shown in Figs. 3 and 5, there is here a significant size dependence, with the slope of the tail becoming less negative with increasing L. Asymptotically, the slope should be given by Eq. (21), which has the value $-2/3$ using the exponent values obtained earlier.[10] The $L=6$ data have a slope of -1.7 and the $L=12$ a slope of -0.95 so it is possible that the slope would tend to $-2/3$ for $L\to\infty$. However, it is also possible that the slope might be less negative then this, which would imply a value of z larger than 3/2.

VI. GLOBAL NONLINEAR SUSCEPTIBILITY

Experimentally[9] one measures the *global* nonlinear susceptibility, for which the local magnetization $\langle\sigma_i^z\rangle$ in (7) and the local external field h_i have to be replaced by the mean global magnetization, $L^{-d}\Sigma_i\langle\sigma_i^z\rangle$ and a uniform field, H, respectively. For the effective classical model this means that one has to consider

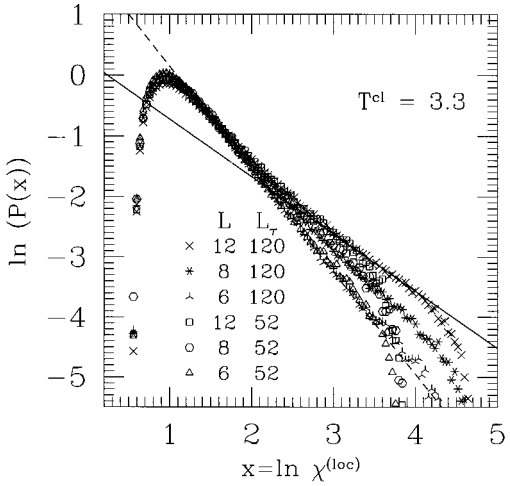

FIG. 10. High precision data with large L_τ for the distribution of the local susceptibility at the critical point, $T^{\mathrm{cl}}=3.30$. The number of samples was 25600 for $L=6$ and 10240 for $L=8$ and 12. The dashed line, which is a fit to the $L=6$ data, has a slope of -1.7, and the solid line, which is a fit to the $L=12$ data, has a slope of -0.95. Using the values of exponents found earlier (Ref. 10) the slope, given by Eq. (21), is expected to be about $-2/3$ in the thermodynamic limit, and it is certainly plausible that data for larger sizes would extrapolate to this value.

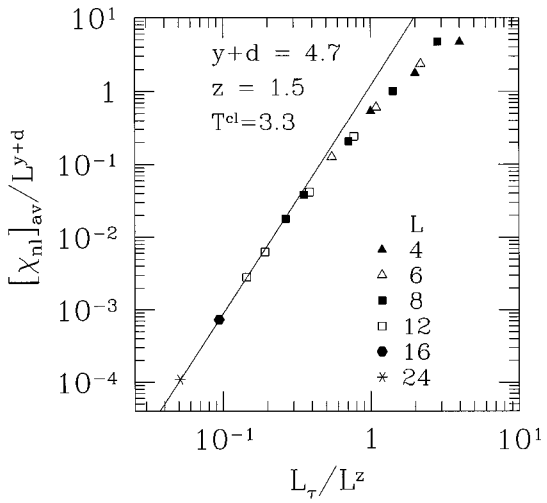

FIG. 11. A plot of the average global nonlinear susceptibility at criticality, for a range of sizes and aspect ratios. The exponents used in this fit are $z=1/5$ and $y+d=4.7$. In earlier work (Ref. 10), we found $z\simeq 1.5$, $y+d\simeq 4.5$ so the present results are consistent with these estimates. In the limit $L_\tau \ll L^z$, the average global nonlinear susceptibility varies as $L_\tau^{(d+y)/z}\sim T^{-(d+y)/z}$ giving a strong divergence of roughly $T^{-3.1}$. This behavior is shown by the solid line, which is a fit to the data for small L_τ/L^z and has slope 3.1.

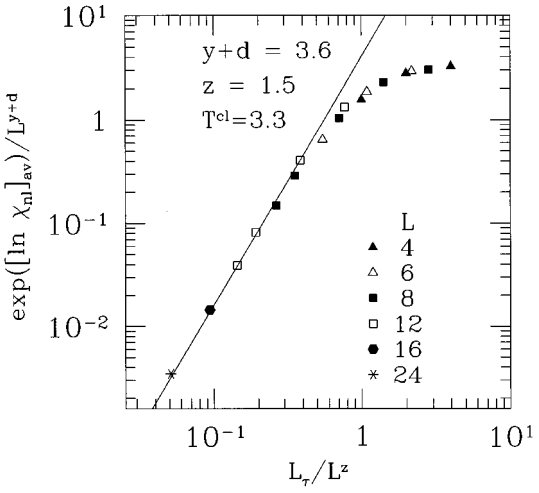

FIG. 12. A plot of the typical global nonlinear susceptibility, defined in Eq. (36), at criticality, for a range of sizes and aspect ratios. In the limit $L_\tau \ll L^z$, the typical global nonlinear susceptibility varies as $L_\tau^{(d+y)/z}\sim T^{-(d+y)/z}$ giving a quite strong divergence of roughly $T^{-2.4}$. This behavior is shown by the solid line, which is a fit to the data for small L_τ/L^z and has slope 2.4.

$$\chi_{\rm nl}=-\frac{1}{6L_\tau L^d}(\langle M^4\rangle-3\langle M^2\rangle^2) \tag{33}$$

with $M=\Sigma_{i,\tau}S_i(\tau)$. In earlier work[10] we found that this quantity diverges at criticality (for fixed aspect ratio) like $\chi_{\rm nl}\sim L^{y+d}$, with y given by (31), so for arbitrary aspect ratio, finite size scaling gives

$$[\chi_{\rm nl}]_{\rm av}=L^{y+d}\tilde{\chi}_{\rm nl}\left(\frac{L_\tau}{L^z}\right), \tag{34}$$

at criticality. Here, we have looked at scaling of various moments of the global nonlinear susceptibility *at the critical point*, for a range of aspect ratios. For example the average is shown in Fig. 11. Since there are two exponents which can be adjusted, y and z, the data are unable to determine them both with precision. However, in the limit $L_\tau/L^z\ll 1$, where the dependence on L drops out and

$$[\chi_{\rm nl}]_{\rm av}\sim L_\tau^{(d+y)/z}\sim T^{-(d+y)/z}, \tag{35}$$

the data constrain $(d+y)/z$ to be about 3, in agreement with the T^{-3} divergence at criticality found in earlier work.[10] Figure 11 assumes the previously determined value of z, i.e., $z=1.5$.

In addition we have evaluated the *typical* global nonlinear susceptibility defined by

$$\chi_{\rm nl}^{\rm typ}=\exp[\ln\chi_{\rm nl}]_{\rm av}, \tag{36}$$

at the critical point and show the data in Fig. 12. As with the data for the average in Fig. 11, the ratio $(d+y)/z$ is more tightly constrained than either z or $d+y$ separately. A good fit is obtained with $(d+y)/z\simeq 2.4$, which leads to a divergence of roughly $T^{-2.4}$, not quite so strong as from the average nonlinear susceptibility. The difference may well reflect corrections to scaling for the range of sizes that we were able to study. Note that even the typical value has a strong divergence with T at criticality, in contrast to the experiments.[9]

We have also studied the probability distribution $P(\chi_{\rm nl})$ in the disordered phase. This shows a slightly more complicated behavior than the probability distribution of local quantities presented above. We find that the power describing the tail in the same distribution is the same as that of the local nonlinear susceptibility. This is reasonable since these unusually large values come from correlations which are very long ranged in time, whereas the spatial correlation length is small and so does not give a significant extra effect. These spatial correlations do, however, cause the peak in the distribution to shift to larger values with increasing system size, though presumably the peak position would eventually settle down to a constant for sizes greater than the correlation length.

VII. CONCLUSIONS

One can characterize Griffiths singularities in the disordered phase of a quantum system undergoing a $T=0$ transition with discrete broken symmetry, by a single, continuously varying, dynamical exponent, z. Average response functions may or may not diverge in part of the disordered phase near the critical point, depending on the value of z; see Eqs. (15) and (16). The numerical results, summarized in Fig. 7 and Eqs. (25) and (26), indicate that the average linear susceptibility does not diverge in the disordered phase of the 2D quantum Ising spin glass, though it diverges at the critical point. The average nonlinear susceptibility *does*, however, diverge in part of the disordered phase.

Numerically, as one approaches the critical point from the disordered phase, the value of z is close to the value obtained precisely at the critical point, see Fig. 7. Since the same result is known to hold exactly in 1D, where they are both

equal to infinity,[4] one might speculate that they are equal in general, though we are not aware of any proof of this. Presumably the detailed dependence of z with $T^{\rm cl}$ in the disordered phase, shown in Fig. 7, is nonuniversal. However, it is interesting to ask whether the answer to the question ''*Does the non-linear susceptibility diverge in the disordered phase*'' is universal or not. From Eq. (16) this depends on whether $z > d/3$ as the critical point is approached. If this limit for z is precisely the same as the value of z at criticality, then the answer to the question *is* universal. However, as we just mentioned, we are not aware of any argument which shows that these two values of z should be equal in general.

A related study has also been carried out recently by Guo *et al.*[12,17] Their results for the 2D spin glass are consistent with ours, and they also performed some simulations for the 3D spin glass. In three dimensions the classical model has a finite temperature transition,[14] so the spin glass phase would exist for a finite range of T, which shrinks to zero as $T^{\rm cl} \to T_c^{\rm cl-}$, see Fig. 1. The results of Guo *et al.*[12] indicate that, in three dimensions, the range of the Griffiths phase over which the nonlinear susceptibility diverges, i.e., the region between $T_c^{\rm cl}$ and $T_{\chi{\rm nl}}^{\rm cl}$ in Fig. 1, is very small but apparently nonzero. It is interesting to speculate on whether the possible divergence of the nonlinear susceptibility in part of the disordered phase might be related to the difference between the experiments[9] which apparently do not find a strong divergence of $\chi_{\rm nl}$ at the quantum critical point, and the simulations[10,11] which do.

The data presented here are consistent with our earlier results[10] in finding a dynamic exponent at the critical point of about 1.5. This is rather different from the situation in one dimension[6,4] where $z = \infty$, and one might ask whether the true dynamical exponent might not be larger than 1.5 in two dimensions, and possibly infinite. While the data for the modest range of sizes that can be studied by Monte Carlo simulations are consistent with a small value of z, we cannot completely rule out the possibility that this estimate would increase if one could study larger sizes. Unfortunately, it does not seem feasible to study very much larger sizes with current computer power, unless a more sophisticated algorithm can be found than the single spin-flip approach used here. Assuming that z is indeed finite, the critical scaling in the two-dimensional quantum Ising spin glass is of a fairly conventional, but anisotropic, type, with z playing the role of an anisotropy exponent. The difference from a classical magnet with anisotropic scaling is that Griffiths singularities give additional singularities in various scaling functions in the limit $L_\tau \gg L^z$, or equivalently $TL^z \ll 1$.

ACKNOWLEDGMENTS

The work of A.P.Y. has been supported by the National Science Foundation under Grant No. DMR-9411964. The work of H.R. was supported by the Deutsche Forschungsgemeinschaft (DFG) and he thanks the Physics Department of UCSC for the kind hospitality. We should like to thank R. N. Bhatt, M. Guo, D. A. Huse, and D. S. Fisher for helpful discussions.

[1] R. B. Griffiths, Phys. Rev. Lett. **23**, 17 (1969).
[2] A. B. Harris, Phys. Rev. B **12**, 203 (1975).
[3] B. M. McCoy, Phys. Rev. Lett. **23**, 383 (1969); Phys. Rev. **188**, 1014 (1969). This work was simultaneous with that of Griffiths and so it has been proposed that quantum Griffiths singularities should be called ''Griffiths-McCoy singularities'' [B. M. McCoy (private communication)]. While this proposal is reasonable, usage of the term ''Griffiths singularities'' is sufficiently entrenched that we continue to use it here.
[4] D. S. Fisher, Phys. Rev. Lett. **69**, 534 (1992); Phys. Rev. B **51**, 6411 (1995).
[5] B. M. McCoy and T. T. Wu, Phys. Rev. **176**, B631 (1968); **188**, 982 (1969).
[6] R. Shankar and G. Murphy, Phys. Rev. B **36**, 536 (1987).
[7] A. P. Young and H. Rieger, Phys. Rev. B (to be published).
[8] M. J. Thill and D. A. Huse, Physica A **15**, 321 (1995).
[9] W. Wu, B. Ellmann, T. F. Rosenbaum, G. Aeppli, and D. H. Reich, Phys. Rev. Lett. **67**, 2076 (1991); W. Wu, D. Bitko, T. F. Rosenbaum, and G. Aeppli, *ibid.* **71**, 1919 (1993).
[10] H. Rieger and A. P. Young, Phys. Rev. Lett. **72**, 4141 (1994).
[11] M. Guo, R. N. Bhatt, and D. A. Huse, Phys. Rev. Lett. **72**, 4137 (1994).
[12] M. Guo, R. N. Bhatt, and D. A. Huse, following paper, Phys. Rev. B **54**, 3336 (1996).
[13] For a review on transverse field Ising models, see B. K. Chakrabarti, A. Dutta, and P. Sen, *Quantum Ising Phases and Transitions in Transverse Ising Models*, Lecture Notes in Physics Vol. M41 (Springer-Verlag, Berlin, 1996), and references therein.
[14] K. Binder and A. P. Young, Rev. Mod. Phys. **58**, 801 (1986).
[15] M. Randeira, J. P. Sethna, and R. G. Palmer, Phys. Rev. Lett. **54**, 1321 (1985).
[16] A. J. Bray, Phys. Rev. Lett. **60**, 720 (1988).
[17] M. Guo, Ph.D. thesis, Princeton University, 1995.